LETTER

doi:10.1038/nature11517

The molecular basis of phosphate discrimination in arsenate-rich environments

Mikael Elias[1]*, Alon Wellner[1]*, Korina Goldin-Azulay[1], Eric Chabriere[2], Julia A. Vorholt[3], Tobias J. Erb[3] & Dan S. Tawfik[1]

Arsenate and phosphate are abundant on Earth and have striking similarities: nearly identical pK_a values[1,2], similarly charged oxygen atoms, and thermochemical radii that differ by only 4% (ref. 3). Phosphate is indispensable and arsenate is toxic, but this extensive similarity raises the question whether arsenate may substitute for phosphate in certain niches[4,5]. However, whether it is used or excluded, discriminating phosphate from arsenate is a paramount challenge. Enzymes that utilize phosphate, for example, have the same binding mode and kinetic parameters as arsenate, and the latter's presence therefore decouples metabolism[6,7]. Can proteins discriminate between these two anions, and how would they do so? In particular, cellular phosphate uptake systems face a challenge in arsenate-rich environments. Here we describe a molecular mechanism for this process. We examined the periplasmic phosphate-binding proteins (PBPs) of the ABC-type transport system that mediates phosphate uptake into bacterial cells, including two PBPs from the arsenate-rich Mono Lake *Halomonas* strain GFAJ-1. All PBPs tested are capable of discriminating phosphate over arsenate at least 500-fold. The exception is one of the PBPs of GFAJ-1 that shows roughly 4,500-fold discrimination and its gene is highly expressed under phosphate-limiting conditions. Sub-ångström-resolution structures of *Pseudomonas fluorescens* PBP with both arsenate and phosphate show a unique mode of binding that mediates discrimination. An extensive network of dipole–anion interactions[8,9], and of repulsive interactions, results in the 4% larger arsenate distorting a unique low-barrier hydrogen bond. These features enable the phosphate transport system to bind phosphate selectively over arsenate (at least 10^3 excess) even in highly arsenate-rich environments.

Phosphate transport is mediated by two distinct systems in bacteria and archaea: the phosphate inorganic transport (Pit), a low-affinity and low-selectivity system operating at high phosphate concentrations[10], and the phosphate-specific transport (Pst)[10]. The latter is a high-affinity and high-selectivity ATP-fuelled transporter operating at low phosphate concentration[11] and in high arsenate conditions[10,12]. It comprises a periplasmic high-affinity PBP (or pstS) whose K_d for phosphate is in the submicromolar range[13]. The PBP-captured phosphate anion is subsequently transported across the membrane by an ABC transporter that is energized by ATP to transfer phosphate against the concentration gradient[11]. We examined five bacterial PBPs for their discrimination of phosphate from arsenate. Two PBPs came from arsenate-sensitive species (*Escherichia coli and P. fluorescens*), and the other three came from arsenate-resistant bacteria: *Klebsiella variicola* from Lake Albano (Italy)[14] and the highly arsenate-resistant bacterium *Halomonas* sp. GFAJ-1 (Mono Lake, USA), for which controversy exists over whether it incorporates arsenate into its DNA[5] or not[15,16]. The genome of the latter contains two pstS paralogues from two distinct *pst* operons belonging to so-called 'arsenic islands'[17]. To what degree do these five PBPs distinguish between phosphate and arsenate? What is the molecular basis of their discrimination? Do PBPs adapt to arsenate-rich environments by evolving higher selectivity for phosphate, or perhaps by divergence to import arsenate under certain circumstances?

The five PBPs studied share little sequence identity (Supplementary Fig. 1 and Supplementary Table 1). However, the two *Halomonas* GFAJ-1 PBPs are closely related (Supplementary Fig. 2), and one of them, PBP-2, resides in a phylogenetic clade that comprises extremophiles, and in particular high-salt-resistant and arsenate-resistant organisms (Supplementary Fig. 3 and Supplementary Table 2). We cloned, purified and characterized these five PBPs (Supplementary Information). Despite being isolated from very different sources, four PBPs discriminated phosphate from arsenate 500–850-fold. The exception was the *Halomonas* GFAJ-1 PBP-2 paralogue, which showed much higher discrimination (at least 4,500-fold; Fig. 1a and Supplementary Table 3). Both PBPs of *Halomonas* GFAJ-1 showed specificity for phosphate, which ruled out the possibility that one of them had diverged to serve in arsenate transport. However, the presence of two PBPs raised the question of which of them might be active under phosphate-limiting (and in particular arsenate-rich) environments. Analysis of messenger RNA levels showed that PBP-2 is upregulated more than 40-fold and highly expressed at limiting phosphate concentrations (10 μM), whereas PBP-1 shows barely detectable expression that is only moderately affected by the phosphate level independent of the presence or absence of arsenate (Supplementary Tables 4a, b and 5).

All PBPs have a similar fold that consists of two structurally similar domains linked by a flexible hinge[9] (Supplementary Fig. 4a, b). In the closed form, the binding pocket is buried between the domains and the bound ion is totally dehydrated and completely sequestered. The structure opens to release its cargo anion on binding the transporter. Dipole–ion hydrogen bonds underline the high selectivity of PBPs[18–21] as manifested in the reported 10^5-fold discrimination of phosphate over sulphate[8,9,22]. In both *E. coli* and *P. fluorescens* PBP (the latter dubbed PfluDING), phosphate is bound through 12 hydrogen bonds, of which 9 are ion–dipole interactions: 5 backbone NH groups and 4 hydroxyl groups of serine and threonine (Supplementary Fig. 5).

Phosphate and sulphate differ significantly, not only in having three and two ionizable oxygens, respectively (the structure of sulphate is $(O=)_2S-O_2^{2-}$), and in having different pK_a values, but also in size[3]. Indeed, sulphate and similar anions such as iodate are readily distinguished by phosphate-using enzymes[23]. It is less clear, however, how the far more similar phosphate and arsenate are discriminated. In fact, the differences between their binding interactions are so subtle that they could only be unravelled in sub-ångström-resolution structures obtained for the arsenate-bound PfluDING at pH 4.5 and 8.5 (Supplementary Tables 7 and 9; PDB 4F19 and 4F18; 0.95 and 0.96 Å resolution, respectively). The arsenate structures were compared with the equivalent structures with phosphate (Supplementary Tables 8 and 9; PDB 4F1U and 4F1V; 0.98 and 0.88 Å resolution, respectively). Besides the observable difference in the electronic content of phosphorus and arsenic atoms (15 versus 33 electrons), the substitution of phosphate by arsenate was verified by anomalous scattering X-ray

[1]Department of Biological Chemistry, Weizmann Institute of Science, Rehovot 76100, Israel. [2]Unité de recherche sur les maladies infectieuses et tropicales émergentes, Faculté de Médecine et de Pharmacie, CNRS-Université de la Méditerranée, 13385 Marseille, France. [3]Institute of Microbiology, Eidgenössische Technische Hochschule Zurich, Wolfgang Pauli Strasse 10, 8093 Zurich, Switzerland.
*These authors contributed equally to this work.

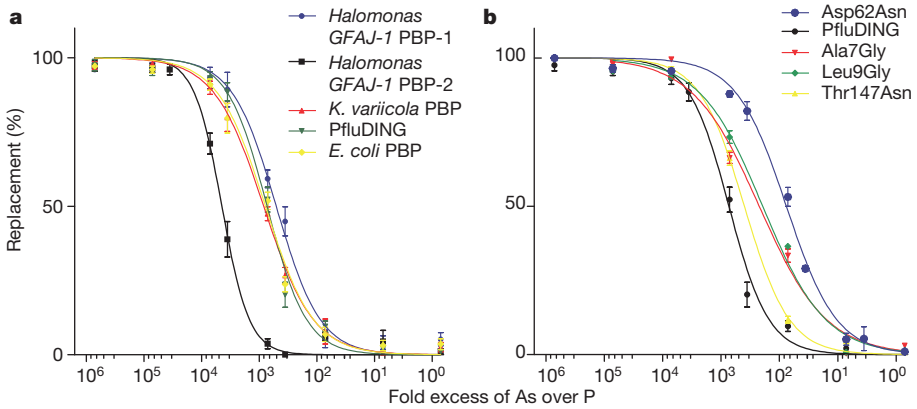

Figure 1 | The phosphate–arsenate selectivity of PBPs. **a**, PBPs were equilibrated with radiolabelled phosphate and varying arsenate concentrations (0.1 μM to 100 mM). The level of radioactivity (that is, of protein-bound phosphate) with no arsenate corresponded to 0% replacement. *Halomonas* PBP-2 was also found to have higher selectivity for vanadate and sulphate (Supplementary Fig. 12). **b**, The phosphate–arsenate selectivity of PfluDING mutants. The mutation Thr147Asn decreased phosphate binding[18] but hardly affected selectivity. In contrast, mutations in the residues mediating unfavourable interactions (Ala7Gly and Leu9Gly), and mutation Asp62Asn altering the short hydrogen bond, decreased selectivity between fourfold and tenfold (see also Supplementary Figs 9 and 10). Details of the curve fitting and the inferred discrimination factors are provided in Supplementary Tables 3 and 14. Error bars show s.e.m. calculated with two to four independent repeats.

diffraction (Supplementary Table 10 and Supplementary Fig. 6). As observed in arsenate-bound enzyme structures[23,24], the arsenate binds in exactly the same mode as phosphate, and the side chains of the protein within the binding cleft superimpose perfectly (Fig. 2a). Further, the hydrogen locations as determined from the high-quality electronic density maps (Fig. 2b and Supplementary Fig. 7) reveal that, as expected from their identical pK_a values, arsenate and phosphate are both bound in their dibasic forms ($H(As/P)O_4^{2-}$) at both pH 4.5 and pH 8.5 (also confirmed by As–O bond lengths; Supplementary Table 11). This feature—the binding of dibasic phosphate at pH 4.5—was attributed to the unusually high number of hydrogen bonds that solvate the bound anion[22] and to a specific charge network in *Mycobacterium tuberculosis* PBP[21]. Finally, the differences in P–O and As–O bond lengths (0.08–0.14 Å) barely perturb the donor–acceptor hydrogen bond distances (D–H) and angles (Supplementary Tables 11–13). How, then, is arsenate discriminated against?

The only significant difference that we could observe between the arsenate-bound and phosphate-bound structures resided in the remarkably short interaction distance (about 2.50 Å) from the carboxylate of Asp 62 to O2 of the anions, a proposed key interaction for specificity[8,21,25]. This distance is typical of low-barrier hydrogen bonds (LBHBs)[26], and is specifically categorized as a heteromolecular negative-charge-assisted hydrogen bond ((−)CAHB). The shared hydrogen atoms involved in these bonds are rarely observable by diffraction techniques because of their diffuse character[27]. Nonetheless, the high resolution and quality of our structures allowed the shared proton to be located, although at relatively low signal-to-noise ratios (Fig. 3). In the phosphate complex, the hydrogen atom occupies a nearly central position at pH 8.5 (D–H 1.19 Å; Fig. 3a and Supplementary Table 13) but not at pH 4.5 (Supplementary Table 12), as expected for optimal CAHBs. In the arsenate-bound structure, this short donor–acceptor distance is maintained (2.50 Å). However, the

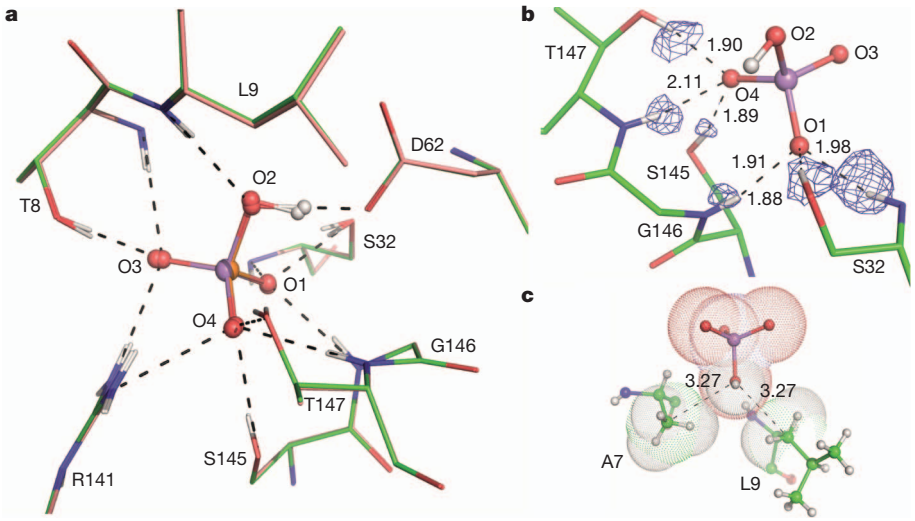

Figure 2 | Binding of arsenate and phosphate to PfluDING. **a**, Superimposition of the arsenate-bound (green sticks; PDB 4F18; pH 8.5) and phosphate-bound (pink sticks; PDB 4F1V; pH 8.5) PfluDING structures. The arsenate (red and violet spheres) and phosphate (orange and red spheres) superimpose perfectly, as do all protein residues. Hydrogen bonds underlining the bound anion are shown as black dashes. **b**, Key ion–dipole interactions in the arsenate structure. Residues involved in the binding (green sticks) donate hydrogen atoms (white sticks, revealed by the omit-H Fourier difference map (blue mesh) contoured at 2σ) to the bound arsenate ion. **c**, Unfavourable contacts between the arsenate ion (red and violet) and the Cβ atoms of Ala 7 and Leu 9 (see also Supplementary Fig. 13). The van der Waals radii are shown as dashes. Distances are indicated in ångströms (standard deviations are available in Supplementary Tables 13 and 11).

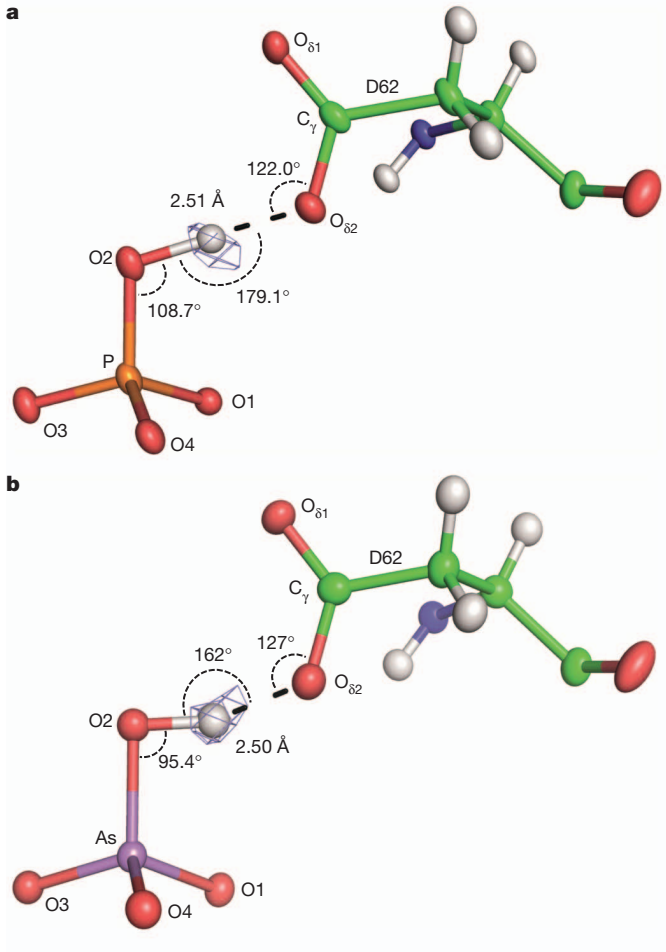

Figure 3 | The (−)CAHB angles are optimal in the phosphate-bound structure but distorted with arsenate. **a**, A close-up view of the short hydrogen bond ((−)CAHB, or LBHB) between O2 of the bound phosphate and the carboxylate of Asp 62 (pH 8.5; PDB 4F1V). The shared hydrogen atom is revealed by the omit-H Fourier difference map (blue mesh) contoured at 2.5σ (peak height 3.3σ). **b**, The same bond in the arsenate-bound structure, with the omit-H Fourier difference map (blue mesh) contoured at 1.4σ (peak height 1.9σ; the pH 4.5 structure is presented for clarity). Noted are the bond lengths and the angles of the short hydrogen bonds. Atoms are represented as their anisotropic thermal ellipsoids. Measurements made in structures at both pH values (4.5 and 8.5) and corresponding standard deviation values are available in Supplementary Tables 11–13. Alternative models are presented in Supplementary Fig. 8.

proton is asymmetrically located at both pH values (D–H ≈ 1.08 Å), suggesting a weaker interaction (Supplementary Tables 12 and 13).

The three angles that define the CAHB are nearly canonical in the phosphate structure (P–O2–H = 108.7°; O2–H···$O_{\delta2}$ = 179.1°; C_γ-$O_{\delta2}$···H = 122°; which are all ±2° from the canonical angles). However, these angles are all suboptimal for the bound arsenate (As–O2–H = 95.4°; O2–H···$O_{\delta2}$ = 162°; C_γ–$O_{\delta2}$···H = 127; Fig. 3 and Supplementary Tables 11–13). This distortion is the consequence of the longer As–O2 bond than the P–O2 bond (Supplementary Fig. 8b), and may readily account for the difference of about 500-fold in favour of phosphate binding. We note that even when the shared hydrogen was modelled with the canonical As–O2–H angle, and not according to the observed residual density, the remaining two angles were severely distorted (Supplementary Fig. 8a).

The distorted bonding angles with Asp 62 suggest that the primary contribution of Asp 62 is not in anion binding itself. Indeed, the mutation Asp81Asn in *E. coli* PBP (equivalent to Asp62Asn) showed no effect on phosphate binding[25]. However, we found that this mutation, in PfluDING, significantly disturbed the discrimination against arsenate (about tenfold; Fig. 1b and Supplementary Table 14). The equivalent mutation in *E. coli* PBP gave a similar decrease in arsenate discrimination (Supplementary Fig. 9) and an even greater effect with sulphate (about 100-fold; Supplementary Fig. 10). Conversely, a mutation that affected the phosphate-binding ability (Thr147Asn)[18] had little effect on the discrimination (Fig. 1b and Supplementary Table 14). The energy of this short bond may therefore be channelled not towards anion-binding affinity but rather towards anion selectivity.

In that conformational flexibility mediates promiscuity[28], the high selectivity of PBPs relies on structural rigidity. This rigidity relates to the protein's conformation as well as extremely precise positioning and tight packing of the phosphate[21]. The former is illustrated by an analysis of *B*-factors of the region of the binding site (Supplementary Table 15). Moreover, most H-donor groups are backbone NH groups coming from the first turns of α-helices, or from residues with a short side chain (serine or threonine) whose rotameric states are fixed by a network of hydrogen bonds. In addition to the extensive constellation of anion–dipole interactions, the bound anions are also immobilized by tight van der Waals interactions. The O2 of the phosphate is equidistant (3.35 Å) from the Cβ atoms of Ala 7 and Leu 9, thus resulting in two short, unfavourable interactions (Fig. 2c). These distances are smaller than the sum of the van der Waals radii (1.92 Å (radius of CH_2 and CH_3) plus 1.54 Å (radius of OH)[29] = 3.46 Å) and become even shorter (and thus more unfavourable) with arsenate (3.27 Å; values for pH 8.5 structures are given in Supplementary Table 11). Although not previously noted, these interactions seem to be conserved in PBPs (Supplementary Fig. 11). Accordingly, the mutations of either Ala 7 or Leu 9 into glycine that may eliminate these repulsive interactions resulted in a marked decrease in arsenate discrimination (about fourfold; Fig. 1b and Supplementary Table 14).

Taken together, our data indicate that PBPs show exquisite selectivity with respect to arsenate, whereas phosphate-binding proteins tested so far, enzymes and transporters alike, show no or low selectivity[7]. PBPs therefore seem to have evolved a unique mode of binding that is capable of distinguishing between the highly similar phosphate and arsenate. Anion binding is mediated by a dense and rigid network of ion–dipole interactions[9,30]. This network is sensitive to geometric changes. However, the perturbation imposed by the slightly larger arsenate is not equally distributed between all bonds but rather it is channelled almost solely to the short, high-energy hydrogen bond which is most sensitive to both angle and distance perturbations (Fig. 3). The channelling of this unique interaction is the outcome of the extremely tight positioning of the anion, mediated also by unfavourable interactions of the bound anions with two juxtaposed Cβ atoms (Fig. 2c) within a rigid, highly connected binding site (Fig. 2a). Weakening of these interactions (for example by site-directed mutagenesis) significantly decreases the discrimination against arsenate (Fig. 1b); however, at least in the case of the short hydrogen bond, this seems to have little effect on phosphate binding. These structural features therefore support the notion that anion binding and anion selectivity are two independently evolved features.

The notion that PBPs evolved to meet arsenate challenges is also consistent with the observation that the *pst* system seems to be essential for the survival of *E. coli* in arsenate medium[12]. It also seems that the selectivity of bacterial PBPs can be further increased in arsenate-rich environments. The PBP-2 paralogue of *Halomonas* GFAJ-1 showed roughly tenfold higher selectivity than any other bacterial PBP we tested (Fig. 1). PBP-2 also belongs to a phylogenetic clade of high-salt-resistant and arsenate-resistant bacterial species (Supplementary Fig. 3 and Supplementary Table 2). The structural features of this clade and the origin of the high selectivity of PBP-2 remain unknown (Supplementary Fig. 4c, d). However, we note that PBP-2 seems to be functional *in vivo* and is selectively expressed at very low phosphate concentrations (10 μM; Supplementary Tables 4a, b, 5 and 16–18). Finally, the observed discrimination factor for PBP-2, *in vitro* as isolated protein (4,500-fold) is strikingly close to the discrimination levels

in vivo, by which a 4,000-fold excess of arsenate in the medium yielded only a 2.5-fold excess of intracellular arsenate (Supplementary Table 6). Thus, *Halomonas* GFAJ-1 seems to have evolved to extract phosphate[16] and, owing to the unique discrimination mode of its PBP, can do so at arsenate-to-phosphate ratios that are more than 3,000-fold higher than those observed in Mono Lake.

METHODS SUMMARY

Discrimination assays. The five PBPs in this study were cloned, overexpressed in *E. coli* and purified. PBPs were tested for discrimination of phosphate from different anions (arsenate, vanadate and sulphate) by dialyzing them against 50 mM Tris-HCl buffer pH 8.0 containing a total of 140 nM phosphate (with 1 μCi of radiolabelled phosphate, ^{32}P) and increasing concentrations of the competing anion at tenfold serial dilutions (0.1 μM to 100 mM). All experiments were performed with two to four independent repeats and included a control assay without PBP in the dialysis tube. The background absorption rate by 0.1% BSA was over 1,000-fold less than the PBP signal.

Crystallization and diffraction data collection. PfluDING was extensively dialysed against 50 mM Tris-HCl buffer pH 8 containing 10 mM arsenate and 1 mM $CaCl_2$ (to chelate phosphate). Crystals of the arsenate-bound form were subsequently obtained using hanging-drop vapour diffusion as described previously[22], but using 100 mM arsenate solution as buffer at pH 4.5 or 8.5. Diffraction data collections on PfluDING crystals, including anomalous data at the arsenate edge, were performed at the European Synchrotron Radiation Facility (Grenoble, France) at beamlines ID-29 and ID-23-1. For both data collections in Supplementary Table 7, only 180° out of the 360° collected were used for refinement, to minimize the effect of radiation damage.

A complete description of materials and methods is provided in Supplementary Methods.

Received 6 May; accepted 15 August 2012.
Published online 3 October 2012.

1. Kohn, R. A. & Dunlap, T. F. Calculation of the buffering capacity of bicarbonate in the rumen and *in vitro*. *J. Anim. Sci.* **76,** 1702–1709 (1998).
2. Larsen, E. H. & Hansen, S. H. Separation of arsenic species by ion-pair and ion exchange high performance liquid chromatography. *Microchim. Acta* **109,** 47–51 (1992).
3. Kish, M. M. & Viola, R. E. Oxyanion specificity of aspartate-β-semialdehyde dehydrogenase. *Inorg. Chem.* **38,** 818–820 (1999).
4. Westheimer, F. H. Why nature chose phosphates. *Science* **235,** 1173–1178 (1987).
5. Wolfe-Simon, F. *et al.* A bacterium that can grow by using arsenic instead of phosphorus. *Science* **332,** 1163–1166 (2011).
6. Dixon, H. B. F. The biochemical action of arsonic acids especially as phosphate analogues. *Adv. Inorg. Chem.* **44,** 191–227 (1997).
7. Tawfik, D. S. & Viola, R. E. Arsenate replacing phosphate: alternative life chemistries and ion promiscuity. *Biochemistry* **50,** 1128–1134 (2011).
8. Luecke, H. & Quiocho, F. A. High specificity of a phosphate transport protein determined by hydrogen bonds. *Nature* **347,** 402–406 (1990).
9. Quiocho, F. A. & Ledvina, P. S. Atomic structure and specificity of bacterial periplasmic receptors for active transport and chemotaxis: variation of common themes. *Mol. Microbiol.* **20,** 17–25 (1996).
10. Willsky, G. R. & Malamy, M. H. Characterization of two genetically separable inorganic phosphate transport systems in *Escherichia coli*. *J. Bacteriol.* **144,** 356–365 (1980).
11. Rao, N. N. & Torriani, A. Molecular aspects of phosphate transport in *Escherichia coli*. *Mol. Microbiol.* **4,** 1083–1090 (1990).
12. Willsky, G. R. & Malamy, M. H. Effect of arsenate on inorganic phosphate transport in *Escherichia coli*. *J. Bacteriol.* **144,** 366–374 (1980).
13. Quiocho, F. A. Atomic structures of periplasmic binding proteins and the high-affinity active transport systems in bacteria. *Phil. Trans. R. Soc. Lond. B* **326,** 341–351 (1990).
14. Butt, A. & Rehman, A. Isolation of arsenite-oxidizing bacteria from industrial effluents and their potential use in wastewater treatment. *World J. Microbiol. Biotechnol.* **27,** 2435–2441 (2011).
15. Reaves, M. L., Sinha, S., Rabinowitz, J. D., Kruglyak, L. & Redfield, R. J. Absence of detectable arsenate in DNA from arsenate-grown GFAJ-1 cells. *Science* **337,** 470–473 (2012).
16. Erb, T. J., Kiefer, P., Hattendorf, B., Gunther, D. & Vorholt, J. A. GFAJ-1 is an arsenate-resistant, phosphate-dependent organism. *Science* **337,** 467–470 (2012).
17. Kim, E.-H. & Rensing, C. Genome of *Halomonas* strain GFAJ-1, a blueprint for fame or business as usual. *J. Bacteriol.* **194,** 1643–1645 (2012).
18. Ahn, S. *et al.* Structure–function relationships in a bacterial DING protein. *FEBS Lett.* **581,** 3455–3460 (2007).
19. Ledvina, P. S., Yao, N., Choudhary, A. & Quiocho, F. A. Negative electrostatic surface potential of protein sites specific for anionic ligands. *Proc. Natl Acad. Sci. USA* **93,** 6786–6791 (1996).
20. Tanabe, M. *et al.* Structures of OppA and PstS from *Yersinia pestis* indicate variability of interactions with transmembrane domains. *Acta Crystallogr. D* **63,** 1185–1193 (2007).
21. Vyas, N. K., Vyas, M. N. & Quiocho, F. A. Crystal structure of *M.tuberculosis* ABC phosphate transport receptor: specificity and charge compensation dominated by ion–dipole interactions. *Structure* **11,** 765–774 (2003).
22. Liebschner, D. *et al.* Elucidation of the phosphate binding mode of DING proteins revealed by subangstrom X-ray crystallography. *J. Am. Chem. Soc.* **131,** 7879–7886 (2009).
23. Faehnle, C. R., Blanco, J. & Viola, R. E. Structural basis for discrimination between oxyanion substrates or inhibitors in aspartate-β-semialdehyde dehydrogenase. *Acta Crystallogr. D* **60,** 2320–2324 (2004).
24. Kline, P. C. & Schramm, V. L. Purine nucleoside phosphorylase. Catalytic mechanism and transition-state analysis of the arsenolysis reaction. *Biochemistry* **32,** 13212–13219 (1993).
25. Wang, Z., Luecke, H., Yao, N. & Quiocho, F. A. A low energy short hydrogen bond in very high resolution structures of protein receptor–phosphate complexes. *Nature Struct. Biol.* **4,** 519–522 (1997).
26. Cleland, W. W. Low-barrier hydrogen bonds and enzymatic catalysis. *Arch. Biochem. Biophys.* **382,** 1–5 (2000).
27. Steiner, T. & Saenger, W. Lengthening of the covalent O–H bond in O–H···O hydrogen bonds re-examined from low-temperature neutron diffraction data of organic compounds. *Acta Crystallogr. B* **50,** 348–357 (1994).
28. Khersonsky, O. & Tawfik, D. S. Enzyme promiscuity: a mechanistic and evolutionary perspective. *Annu. Rev. Biochem.* **79,** 471–505 (2010).
29. Li, A. J. & Nussinov, R. A set of van der Waals and coulombic radii of protein atoms for molecular and solvent-accessible surface calculation, packing evaluation, and docking. *Proteins* **32,** 111–127 (1998).
30. Pflugrath, J. W. & Quiocho, F. A. Sulphate sequestered in the sulphate-binding protein of *Salmonella typhimurium* is bound solely by hydrogen bonds. *Nature* **314,** 257–260 (1985).

Supplementary Information is available in the online version of the paper.

Acknowledgements We thank G. Gotthard for valuable inputs, C. Jelsch for help with the software Mopro, and A. Toth-Petroczy for help with the phylogenetic analysis. Financial support by the Israel Science Foundation is gratefully acknowledged. M.E. is a fellow supported by the Intra-European Fellowships Marie Curie program (grant No. 252836). D.S.T. is the Nella and Leon Benoziyo Professor of Biochemistry. T.J.E. was supported by an Eidgenössische Technische Hochschule fellowship.

Author Contributions M.E. initiated the project, designed experiments, crystallized the proteins, collected and processed crystallographic data, performed discrimination assays, analysed the data and wrote the manuscript. A.W. cloned, purified and crystallized proteins, performed discrimination assays and analysed data. K.G.A. cloned and constructed the mutants, purified proteins and performed discrimination assays. T.J.E. and J.A.V. designed, performed and analysed reverse transcription PCR, as well as cellular experiments, and provided physiological data. E.C. purified proteins and collected diffraction data. D.S.T. initiated the project, designed experiments, analysed data and wrote the manuscript.

Author Information Coordinates and structure factors for the arsenate-bound PfluDING structures at pH 4.5 and 8.5 are deposited in the Protein Data Bank (accession codes 4F18 and 4F19); the phosphate-bound PfluDING coordinates and structures at pH 4.5 and 8.5 (re-refinement) are deposited in the Protein Data Bank (accession codes 4F1U and 4F1V). Reprints and permissions information is available at www.nature.com/reprints. The authors declare no competing financial interests. Readers are welcome to comment on the online version of the paper. Correspondence and requests for materials should be addressed to D.S.T. (tawfik@weizmann.ac.il) or M.E. (mikael.elias@weizmann.ac.il).